Springer

Journal of
Mechanical
Science and
Technology

Journal of Mechanical Science and Technology 22 (2008) 180~189

www.springerlink.com/content/1738-494x

Investigation of the turbulence characteristics in the swirling flow of a gun-type gas burner with two different hot-wire probes

Jang-Kweon Kim*

Power System Engineering Major Kunsan National University

(Manuscript Received November 10, 2006; Revised May 14, 2007; Accepted July 16, 2007)

Abstract

Mean velocities and turbulence characteristics in the swirling flow of a gun-type gas burner (GTGB) were measured with a triaxial hot-wire probe (T-probe) and compared with previous data measured with an X-type hot-wire probe (X-probe). Vectors and axial mean velocity data obtained by the measurement of the two types of probes in the horizontal plane and in the cross section differ in magnitude, but have very similar shape in overall distribution. Axial mean velocity components show especially wide differences around the slits and outer part of the swirl vanes within the range of X/R=2. Also, various turbulence intensities appear in a similar trend to axial mean velocity components within the range of X/R=2. The radial component of turbulence intensity around the slits and the outer part of swirl vanes above the range of X/R=2 has an opposite phenomenon. On the whole, the T-probe's measurements appear smaller than the X-probe's. This shows that the X-probe is better than the T-probe, especially on the swirling flow because it is much easier to use.

Keywords: Gun-type gas burner (GTGB); Hot-wire anemometer (HWA); Slit; Subsonic wind tunnel; Swirl flow; Swirl vane; Triaxial hot-wire probe (T-probe); X-type hot-wire probe (X-probe)

1. Introduction

A gun-type gas burner (GTGB), consisting of a baffle plate, swirl vanes and slits, was applied to a gas furnace. Swirl vanes were mounted radially on the conical baffle plate to cause a rotational motion into the central part of the GTGB, and slits were mounted radially around the outside of swirl vanes to form jets to the axial flow. With this configuration, the GTGB produces a swirling flow. A swirling flow forms a recirculation zone and high turbulence because it produces an adverse pressure gradient in the axial direction of the burner [1-3]. Moreover, a swirling flow offers a big diffusive capacity that increases entrainment rate and thereby promotes mixing of fuel and air by large increments. A swirling flow is widely used in gas turbines or industrial boilers etc., because it shortens the length of flames and enables a lean burn through the stabilization of flames [4, 5].

It has been shown that the behavior of swirling flow is better controlled by streamlined curvature, centrifugal acceleration and turbulence transport than by a pressure effect [6]. Especially, the recirculation zone in a swirling flow has a reverse flow because the above three kinds of effects cause a vortex breakdown phenomenon equivalent to the abrupt deceleration of the axial velocity component in the central part of flow. It is reported that the recirculation zone increases the entrainment rate and mixing, because the flow becomes unstable with helical disturbances - a type of instability caused by centrifugal force [3, 7]. As a result, it is known that the axial mean velocity component obtained experimentally in a swirling flow is distributed like a wake at the jet axis, with its local maximum value at a certain radius. However, if the flow is far away from the jet exit, these phenom-

*Corresponding author. Tel.: +82 63 469 1848, Fax.: +82 63 469 1841
E-mail address: flowkim@kunsan.ac.kr
DOI 10.1007/s12206-007-1022-9

ena disappear [7].

Such swirling flow phenomena are directly measured and analyzed through flow visualization technique or particle image velocimetry (PIV) or computational fluid dynamics (CFD), etc., and can be indirectly measured and analyzed through a laser-Doppler anemometer (LDA) or hot-wire anemometer (HWA) or multi-hole pressure probe, etc. Here, an HWA is one of the measuring instruments that can easily be used to measure a three-dimensional flow field including swirling flow in an isothermal flow. It is well known that an HWA offers high spatial resolution, lessens flow interference against many kinds of fluid flows and can use a small sized sensor with good sensitivity even in high frequency response and low velocity [8, 9]. An HWA frequently is preferred because it can measure turbulence characteristics more correctly and economically than any other measuring instrument.

Most HWA's sensors that are used to measure three-dimensional flow and turbulence characteristics are known as inclined I-type hot-wire probe (I-probe), X-type hot-wire probe (X-probe) and triple hot-wire probe (T-probe), etc. However, because an inclined I-probe or X-probe necessarily must be rotated to exactly the same measurement position to get mean velocities of each directional component and turbulence characteristics on three-dimensional flow fields, a useful measurement cannot be carried out from one position at a time. Also, when these probes are rotated, infinitesimally different results in magnitude of the axial velocity component may be obtained because positioning of the probe can be inconsistent. These inconsistencies are mainly due to inaccurate alignment between the flow direction and the probe, or differences in the manufacture of probe support and mounting probe on the traversing unit. On the other hand, even though there is a shortcoming in that the measurement of instantaneous three-dimensional velocities by the T-probe is valid only when a free velocity vector enters through a cone of about 70° [10], if the T-probe is aligned exactly on the defined flow fields, there is an advantage in that the T-probe can easily get more correct information about the flow field than an inclined I-probe or X-probe.

T-probes were successful with many types of flows after Jorgensen [11] published the speed conversion equation of a probe that corrects aerodynamic interference due to probe support that happens whenever vector direction on a probe axis is changed. For example, Gaulier [12] used T-probes to the speed range of airflow in domestic fuel burners.

In this study, a three-dimensional flow field of the GTGB [13] with the geometric swirl number 0.34 and swirl vane angle 24° was measured with the T-probe. Then measurement results obtained by the T-probe were compared with already published data from X-probes [13-15]. The purpose of this study is to grasp correctly how mean velocities and turbulence characteristics react according to each probe in the flow field of the GTGB.

2. Experimental apparatus and method

2.1 Experimental apparatus

Fig. 1 shows the detailed geometric structure of the GTGB used in this experiment. This gas burner, which was developed for gas furnaces with heating capacity of 15000 kcal/hr, consists of a conical baffle plate inclined by 45° on the head of circular tube and eight slits arranged radially at regular intervals to the outer circumference of the baffle plate. This baffle plate was blocked within a diameter of 25 mm, and eight swirl vanes were arranged radially at 45° intervals from a diameter of 25 mm to a diameter of 57.8 mm.

Fig. 2 illustrates the process for measuring three-dimensional turbulent flow fields from the GTGB mounted to the test section of a subsonic wind tunnel by using HWA system. A subsonic wind tunnel consists of a centrifugal blower with 3.75 kW AC motor, diffuser, tranquilization, contraction and test section. An inverter was used to change wind tunnel speed and to make the number of blower rotations fixed. The dimensions of this test section are width 220 mm,

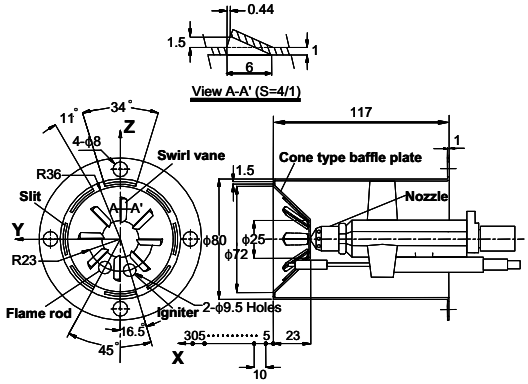

Fig. 1. Configuration of the GTGB.

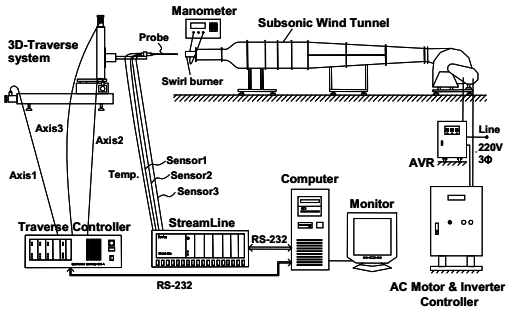

Fig. 2. Experimental apparatus diagram including hot-wire anemometer system.

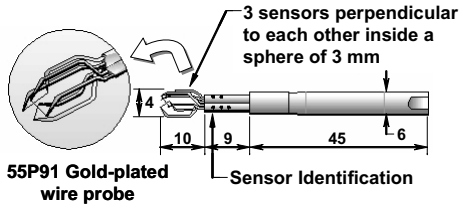

Fig. 3. Configuration of the T-probe.

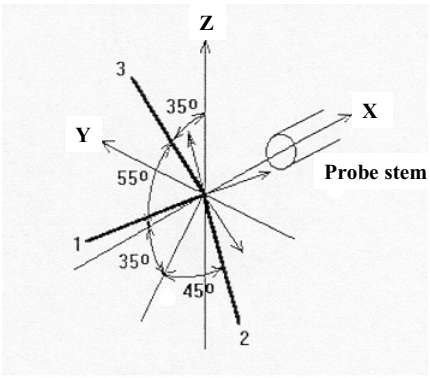

Fig. 4. Relationship between the T-probe and the actual coordinate system.

height 220 mm and length 410 mm. Maximum velocity in the exit of the test section is about 35 m/s, and turbulence intensity is below about 0.02% at about 13 m/s except the edges 20 mm away from the inner wall of the test section. The three-dimensional HWA system (Dantec 90N10 Streamline) used to measure a turbulent flow field in the state of non-combustion consists of a constant temperature-type HWA, speed and direction calibrator (Dantec 90H01 & 90H02), three-dimensional automatic traversing unit (Dantec 41T50 & 41T75) and computer. Here, all of them are linked by RS-232C interface, and the speed calibrator is connected with an air compressor with an effective pressure 10 kg/cm^2.

2.2 Experimental method

2.2.1 Three-dimensional velocity calculation method by the T-probe

In this study, the T-probe (Dantec, 55R91) shown in Fig. 3 was used for the measurement of three-dimensional velocities. The measurement of three-dimensional flow velocities by the T-probe follows [11, 16, 17]; that is, when a T-probe is situated in the three-dimensional space of flow, its axis aligns with the main flow vector as shown in Fig. 4. If velocities that satisfy the wire coordinate system related with three kinds of wires 1, 2 and 3 composing a T-probe are defined as U_1, U_2 and U_3, respectively, and if three-dimensional velocity components for X, Y and Z direction are defined as U, V and W, respectively, the relationship of these velocities is given as Eq. (1) in probe coordinate system satisfying Fig. 4.

$$\begin{aligned} U &= U_1\cos 54.736^\circ + U_2\cos 54.736^\circ + U_3\cos 54.736^\circ \\ V &= -U_1\cos 45^\circ - U_2\cos 135^\circ + U_3\cos 90^\circ \\ W &= -U_1\cos 114.094^\circ - U_2\cos 114.094^\circ - U_3\cos 35.264^\circ \end{aligned} \tag{1}$$

On the other hand, when the cooling effects for tangential direction of wire and interference phenomenon of probe support are considered, if effective cooling velocity on each wire is defined as U_{1eff}, U_{2eff} and U_{3eff}, respectively, and if yaw coefficient and pitch are defined as k_i, h_i, respectively, the velocity components of U_1, U_2 and U_3 for wire coordinate system are given by Eq. (2).

$$\begin{aligned} U_{1eff}^2 &= k_1^2\cdot U_1^2 + U_2^2 + h_1^2\cdot U_3^2 \\ U_{2eff}^2 &= h_2^2\cdot U_1^2 + k_2^2\cdot U_2^2 + U_3^2 \\ U_{3eff}^2 &= U_1^2 + h_3^2\cdot U_2^2 + k_3^2\cdot U_3^2 \end{aligned} \tag{2}$$

Because the T-probe is calibrated with the velocity in the direction of the probe axis, U_{eff} can be replaced as $U_{cal}\cdot(1+k_i^2+h_i^2)^{0.5}\cdot\cos 35.264^\circ$. Here, 35.264° is an angle that the flow velocity forms with a vertical plane to the wires. Therefore, Eq. (2) can be modified again by Eq. (3). That is,

$$\begin{aligned} &U_{1cal}^2\cdot(1+k_1^2+h_1^2)\cdot\cos^2 35.264^\circ \\ &\quad = k_1^2\cdot U_1^2 + U_2^2 + h_1^2\cdot U_3^2 \end{aligned}$$

$$
\begin{aligned}
&U_{2cal}^2 \cdot (1 + k_2^2 + h_2^2) \cdot \cos^2 35.264^\circ \\
&\quad = h_2^2 \cdot U_1^2 + k_2^2 \cdot U_2^2 + U_3^2 \\
&U_{3cal}^2 \cdot (1 + k_3^2 + h_3^2) \cdot \cos^2 35.264^\circ \\
&\quad = U_1^2 + h_3^2 \cdot U_2^2 + k_3^2 \cdot U_3^2
\end{aligned} \tag{3}
$$

If yaw coefficient and pitch for each wire of Eq. (3) through the T-probe's calibration are given, the magnitudes of velocities U_1, U_2 and U_3 for each wire can be obtained easily in Eq. (3). Then, if the magnitudes of velocities for each wire are substituted again for Eq. (1), actual velocity components of U, V and W that satisfy the probe coordinate system of flow can be easily obtained for X, Y and Z directions, respectively.

2.2.2 Velocity measurement method

The exit velocity of the burner in this study was set up under the static pressure of 164 Pa collected from four pressure taps placed on the side of the burner. This static pressure was obtained when an air flow-rate of 450 ℓ/min for combustion was supplied to the burner. The sampling frequency of the A/D converter was 10 kHz per channel, and the sampling number was 102,400 per channel. Also, a low-pass filter of signal conditioner was set up by 30 kHz per channel. Velocity calibration by the T-probe was carried out from 0 m/s to 20 m/s. The resulting velocity calibration accuracy was better than ±1% through the fifth polynomial curve fit analysis.

Direction calibration for Eqs. (2) and (3) was carried out by rotating a probe inclined 30° to the axial flow at 10° intervals from 0° to 350° at constant velocity 10.5 m/s in order to remove the effects of the interference of each wire on rotational flow. For each wire, average yaw coefficients were obtained by $k_1^2 = 0.043$, $k_2^2 = 0.083$ and $k_3^2 = 0.084$, respectively, and average pitch coefficients were obtained by $h_1^2 = 1.07$, $h_2^2 = 1.045$ and $h_3^2 = 1.061$, respectively. All processes can be handled automatically by the built-in software "Streamware" [17].

Next, the T-probe was mounted on an automatic traversing unit, keeping the same direction as when it was set up to the calibrator. Then main velocity measurements were carried out after a correct center point was again determined through the velocity data obtained by traversing a probe finely right and left, or up and down, at the exit plane of the burner in addition to geometric burner center.

As shown in Fig. 1, the GTGB adopted in this study was used after the flame rod and igniter installed to the conical baffle plate was eliminated and after their holes were blocked with adhesive tape. Because the burner shape is symmetrical with regard to the burner's center, velocity measurement positions for X direction and Y direction in the X-Y plane (horizontal plane) at Z=0 mm, under specified air flow-rate conditions for protecting a sensor from the burner exit, were selected at 10mm intervals from 5 mm up to 305 mm and from -70 mm to 70 mm at 5 mm intervals, respectively. Then, measurement positions for radial direction (R) and for rotational direction (θ) in the Y-Z plane (cross section) at X=55 mm distance from the burner exit were selected from 0 mm to 70 mm at 5 mm intervals and from 0° to 355° at 5° intervals, respectively. Here, the fast jet speed spouting out of eight narrow slits was measured in detail by traversing a probe in steps of 1 mm. The indoor temperature of the laboratory was kept steady at 20±0.5℃ to minimize any speed error due to temperature change as much as possible. The change of wind tunnel speed due to line voltage fluctuation was controlled with an automatic voltage regulator.

3. Experimental results and discussions

3.1 Comparison of vector and mean velocity profiles

Fig. 5 shows the vector distribution plotted by mean velocities of each directional component obtained in the X-Y plane with the X-probe and T-probe, respectively. The axial mean velocity component U is displayed together in these pictures. Although the magnitude of mean velocity U distributions shows a small difference between the two probes, the distribution forms of U show similar images on the whole. However, vector distributions show some differences in the vicinity of the slits and outside of the swirl vanes within the range of about X/R=2 equivalent to the relatively initial region, but they have appeared similar in magnitude and direction in other regions. Such differences occur because each probe influences the mean velocities of radial component V and rotational W more greatly than axial mean velocity component U.

Usually, an X-probe can only sense instantaneous velocities when the velocity vectors on the same plane enter by ±45° on a probe axis, but a T-probe can only sense the instantaneous velocities of the conical space inclined about ±35.3° to the probe axis among velocity vectors existing in all planes. As a result,

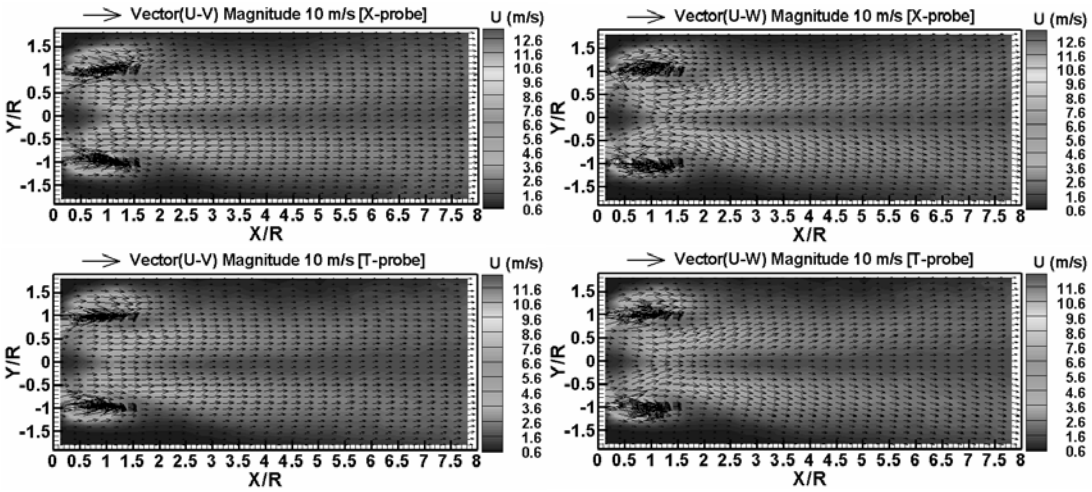

(a) Vector(U-V) Comparison (b) Vector(U-W) Comparison

Fig. 5. Vector and mean velocity contour plot measured in the X-Y plane.

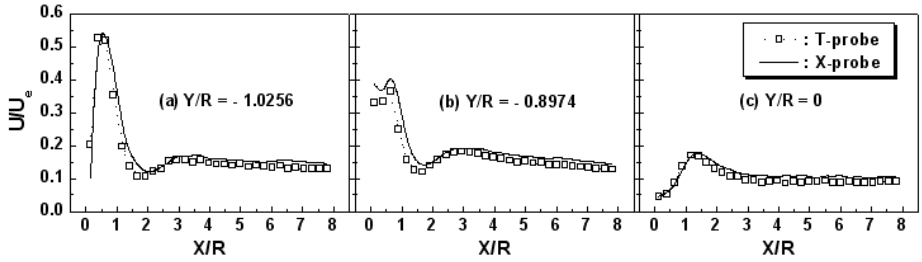

(a) Y/R=-1.0256 (b) Y/R=-0.8974 (c) Y/R=0

Fig. 6. Comparisons of mean velocity U distribution along the downstream distance in the X-Y plane.

because the mixing effect between the fast jet from the slits and the rotational flow from the swirl vanes acts dominantly in the vicinity of the slits and outside of the swirl vanes within the range of about X/R=2, if the spreading angle of flow velocity is beyond the limits of the T-probe's sensing velocity, the values of mean velocities U, V and W may not be properly calculated. Champagne et al. [18] have pointed out that the attack angle of rotational flow affected by a hot-wire probe is less than 45˚ when weak swirling flow has a swirl number less than 0.57. On the other hand, the attack angle in the gas burner [13] used in this study can be expected to be smaller than 45˚ because the swirl vane angle is equal to 24˚ and the geometric swirl number corresponds to 0.34, but it may be beyond the angle of ±35.3˚ equivalent to the sensing extent of the T-probe in some ranges where the spreading effect is large. Therefore, for more correct verification, additional measurements need to be carried out with the LDA or multi-hole pressure probes capable of detecting the flow direction. According to Dantec Dynamics Company's published data, because only three-dimensional rotational flow generally occurs when a helicopter takes off or lands on the deck of an offshore helidrome structure, mean velocities of both longitudinal component and transverse measured by the X-probe were overestimated by 10% relative to those by the T-probe [19].

Fig. 6 shows dimensionless profiles of mean velocity U measured with the X-probe and T-probe, respectively, along the downstream distance at three radial positions. Here, mean velocity U was normalized by maximum burner exit velocity (U_e). Mean velocity U/U_e distributions along the downstream distance show similar curves regardless of the probe's type, in the centerline corresponding to Y/R=0, in the outside of the swirl vanes equivalent to Y/R=-0.8974 and in the vicinity of the slits equivalent to Y/R=-

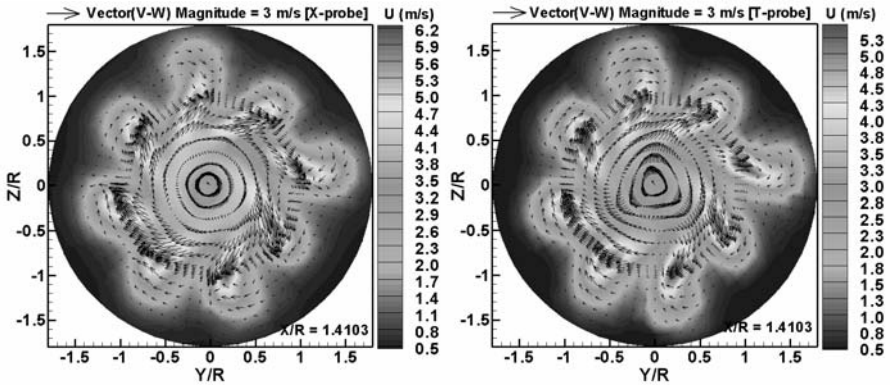

Fig. 7. Vector and mean velocity contour plot measured in the Y-Z plane.

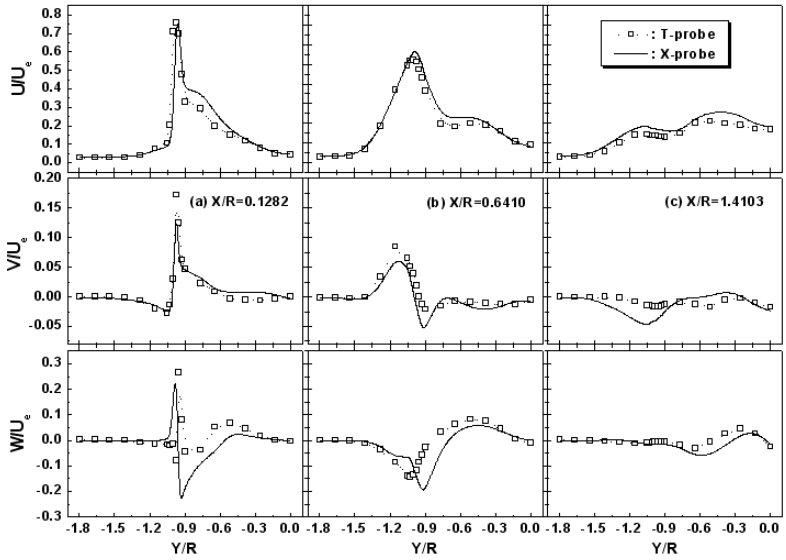

Fig. 8. Comparisons of mean velocity distribution measured in the X-Y plane.

1.0256. However, measurement values from the T-probe in the vicinity of the slits and outside of the swirl vanes within the range of about X/R=2 locally appear about 16% smaller than those from the X-probe. This may be caused by the spreading angle of the swirling flow diffusing at faster speed in the initial region near the burner exit, affecting the two probes differently. Measurement values from the T-probe in other regions have appeared to be about 10% smaller than those from the X-probe.

Fig. 7 shows the contour, including mean velocity U, as well as vector distribution that appears by both radial component V and rotational W measured with the X-probe and the T-probe, respectively, in the Y-Z plane of X/R=1.4103. Mean velocity U shown by the X-probe here is the value calculated by arithmetic mean between two mean velocities obtained when the X-probe was rotated twice. All the mean velocities by the two probes show tiny magnitude differences, but the overall shapes of their distributions are very similar. The fast jet spouted from the vicinity of the slits shows a long hanging image because it is spread by being pushed to the outside by a high centrifugal force created by the rotational flow of the swirl vanes. Also, all vector distributions indicating rotational flow show images that rotate clockwise. However, the rotational direction of the vector formed around the vicinity of the slits appears as measurements by the X-probe extend more to the outside of the burner than those by the T-probe. The vector magnitude clearly

reveals quite a different picture of distribution in the burner central part between the slits. The distributions measured by the X-probe appear relatively circular, while those measured by the T-probe show a triangular form. All things considered, it looks as though the T-probe has a bad sensing resolution to the swirling velocity. It appears that the T-probe is more sensitive to the measuring position than the X-probe. That is, even though we traverse the probe within the very small space such as 0.1 mm in the swirling flow, if we don't match the T-probe to the exact position that we want to measure, some differences in magnitude between the two probes can easily occur.

Fig. 8 shows dimensionless mean velocity profiles of each directional component measured with the X-probe and the T-probe, respectively, according to the distance of Y-axis at the location of X/R=0.1282, 0.6410 and 1.4103 in the X-Y plane. Here, all mean velocities were normalized by maximum burner exit velocity. Because X/R=0.1282 and X/R=0.6410 are equivalent to the initial region where the swirling flow centrifugal effect strongly dominates and a fast jet exists near the slits, mean velocity U/U_e between the slits and the swirl vanes from the X-probe has locally appeared to be about 20% greater than that from the T-probe. Also, X/R=1.4103 being equivalent to the mixed flow region causes the fast jet to be reduced remarkably. The measurement value from the X-probe appears greater on the whole than that from the T-probe except at the edge of burner. On the other hand, because V/U_e and W/U_e appear much smaller than U/U_e and show positive and negative magnitude distributions, one follows a similar curvature distribution to each other between the two probes, another does not. It appears that, when the measurement positions are not exactly identical between the two probes and according to Dantec Dynamics Company's published data, mean velocity measurements by the X-probe were overestimated by 10% relative to those by the T-probe on the rotational flow. In any case, some local differences in velocity magnitude and curvature distribution between the two probes clearly seem to exist here.

3.2 Comparison of turbulence characteristics

Fig. 9 shows the profiles of turbulence intensities of each directional component obtained with the X-probe and the T-probe, respectively, along the downstream distance at three positions of the Y-axis in the X-Y plane. Here, the turbulence intensities are non-dimensionalized values that are ratios of the RMS (root-mean-square) value of each directional fluctuating velocity component to the maximum burner exit velocity. Also, RMS of the fluctuating velocity component u expressed by the X-probe is a value recalculated by arithmetic mean from two RMS values obtained when the probe is rotated two times.

In the two positions Y/R=-0.8974 and Y/R=-1.0256, because the mixing effect between the fast jet spouted by the slits and the rotational motion by the swirl vanes appears to be stronger, all turbulence intensities show greatly different values between the two probes within the range of about X/R=2. However, beyond the range of about X/R=2, turbulence intensities of u/U_e and v/U_e show very similar values. Here, the turbulence intensity u/U_e measured by the T-probe appears a little bit smaller than that measured by the X-probe, while the opposite trend appears in the case of turbulence intensity v/U_e. On the contrary, the turbulence intensity w/U_e of the X-probe shows a greater value than that of the T-probe within the range of about X/R=5. In the case of Y/R=0, corresponding to the centerline, because effects by both the slits and the swirl vanes appear smaller than at other two positions, all turbulence intensities show relatively small values. Here, turbulence intensities of u/U_e and v/U_e of the T-probe appear smaller than those of the X-probe, while the turbulence intensity w/U_e shows almost the same value between the two probes.

Fig. 10 shows the profiles of turbulence intensities of each directional component obtained with the X-probe and T-probe along the Y-axis at three positions, X/R=0.1282, 0.6410 and 1.4103, in the X-Y plane.

Generally, in the flow field of a gas burner like the one used in this study, because the slope of mean velocities of each directional component is formed largely in the vicinity of the slits and outside of the swirl vanes near the range of burner exit, turbulence intensity strongly increases in all directions near the slits and outside of the swirl vanes [13-15].

Turbulence intensities of u/U_e and w/U_e make a difference between the two probes in the vicinity of the slits and outside of the swirl vanes such that great turbulence occurs except at the burner's central part or edge at X/R=0.1282 and X/R=0.6410. Also, their T-probe's values are smaller than the X-probe's. Turbulence intensity v/U_e between the two probes shows a relatively small difference. Remarkably, in

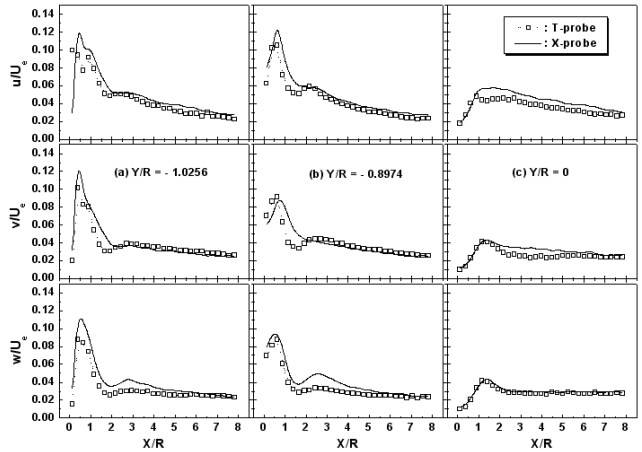

Fig. 9. Comparisons of turbulent intensity distribution along the downstream distance in the X-Y plane.

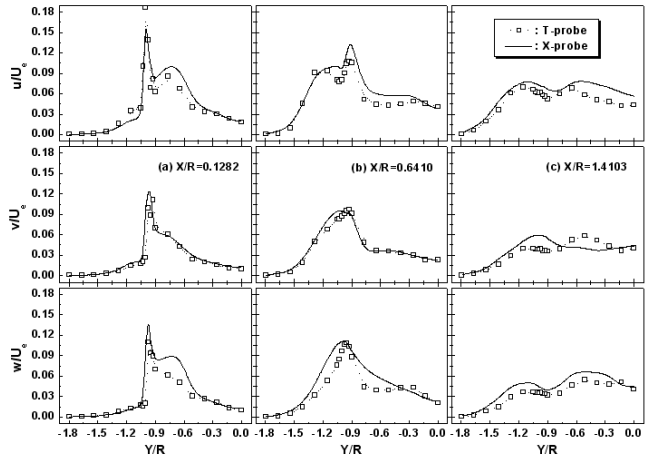

Fig. 10. Comparisons of turbulent intensity distribution measured in the X-Y plane.

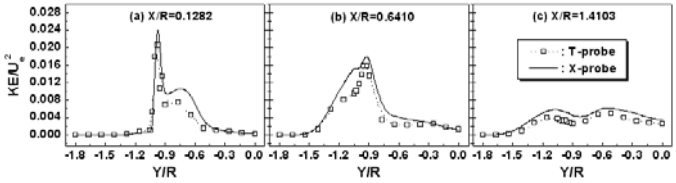

Fig. 11. Comparisons of turbulent kinetic energy distribution measured in the X-Y plane.

the case of the downstream position X/R=1.4103, the independent features between fast jet from the slits and fast rotational flow from the swirl vanes disappear, and the mixed flow feature appears. Therefore, turbulence intensities of u/U_e and w/U_e, obtained by the two probes along the range of all Y-axes (radial) direction, show a similar curved line form, and the T-probe's measurements are smaller than the X-probe's, while the turbulence intensity v/U_e shows a different distribution curve between the two probes.

Fig. 11 shows dimensionless turbulent kinetic energy distributions obtained at three axial positions X/R=0.1282, 0.6410 and 1.4103 in the X-Y plane with the X-probe and T-probe. Here, turbulent kinetic energy is defined as the equation $KE = (u^2 + v^2 + w^2)/2$, and it is normalized by the square of maximum burner exit velocity.

When X/R=0.1282, maximum turbulent kinetic en-

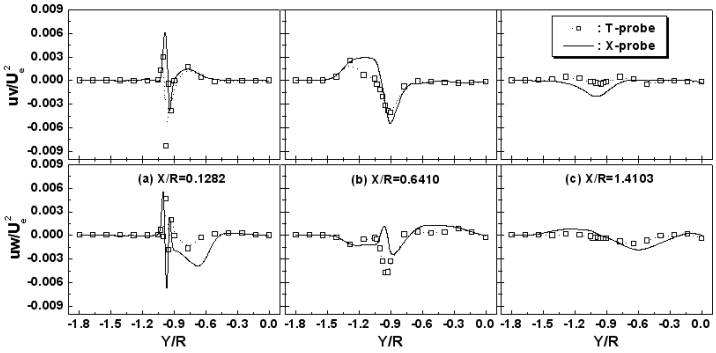

Fig. 12. Comparisons of Reynolds shear stress distribution measured in the X-Y plane.

ergy is formed near the slits, and the T-probe's measurements show some smaller differences in magnitude than the X-probe's, and the gap of measurements between the two probes is larger with a far smaller value in the range of the swirl vanes. Also, with X/R=0.6410, because the magnitude gap between the two probes is much expanded to the outside of the slits, measurements of the T-probe appear to be smaller than those of the X-probe. Conversely, in the case of X/R=1.4103 (that is, a mixed region), turbulent kinetic energy found by the two probes along all Y-axes, except at the burner edge, has a similar curvature distribution, but the T-probe's value appears to be smaller than the X-probe's.

Fig. 12 shows dimensionless turbulent shear stresses obtained with the X-probe and T-probe at three axial positions X/R=0.1282, 0.6410 and 1.4103 in the X-Y plane. Here, these are normalized by the square of maximum burner exit velocity.

All turbulent shear stresses (uv/U_e^2 and uw/U_e^2) between the two probes show positive and negative peak values around the slits at axial position X/R=0.1282 equivalent to the initial region. In the case of uv/U_e^2, measurements by the two probes show similar magnitude distribution and curved line form, except at the slits, but in the case of uw/U_e^2, they show wide differences in the range of the swirl vanes as well as the slits. In particular, when the flow of air goes a little more downstream, turbulent shear stress uv/U_e^2 measured by the T-probe around the slits and the swirl vanes at X/R=0.6410 and X/R= 1.4103 appears to be somewhat smaller than that measured by the X-probe, and shows a curved line distribution of similar curvature between the two probes. On the other hand, uw/U_e^2 shows little difference in curvature or in magnitude between the two probes near the slits and the swirl vanes.

4. Conclusions

In this study, the mean velocities and turbulence characteristics of each directional component from the swirling flow of the GTGB were measured with a T-probe and compared with the results already presented with an X-probe in order to determine the difference of speed response to the type of probe.

Vector distribution and mean velocity U, measured by the two probes in the X-Y plane and Y-Z plane, show a little difference in magnitude, but the whole distribution shows a very similar shape.

Mean velocity U/U_e along the downstream distance shows that measurements by the T-probe locally appear to be about 16% smaller than those by the X-probe around the slits and outside of the swirl vanes within the range of X/R=2, and appear to be about 10% smaller in other ranges. In addition, mean velocity U/U_e along the Y-axis shows that the T-probe's value is locally about 20% smaller than the X-probe's only at X/R=0.1282 and X/R=0.6410.

All turbulence intensities along the downstream distance near the slits within the range of about X/R=2 show different magnitudes between the two probes. However, in the case of X/R>2, even though the absolute magnitudes of all turbulence intensities decrease remarkably, while turbulence intensities of u/U_e and w/U_e measured by the T-probe locally appear to be distributed about 13% smaller than those measured by the X-probe on the average, turbulence intensity v/U_e from the T-probe appears to be about 7% greater than that from the X-probe on the average.

On the whole, all measurement values of the T-probe locally appear smaller than those of the X-probe in regions where the rotational flow dominates,

but their distribution trends are very similar to each other. As a result, the X-probe seems to be better than the T-probe, especially on the swirling flow, because it is much easier to use.

However, even though we admit Dantec Dynamics Company's published data that mean velocity measurements by the X-probe were overestimated by 10% relative to those by the T-probe on rotational flow, we must discriminate between these differences if we believe that a T-probe is more sensitive to the measuring position than an X-probe. In order to reduce the difference in magnitude between the two probes, we must be more careful to find the exact measuring position, especially when we try to measure the swirling flow using a T-probe. In addition, we need to confirm more definitely whether these are the original exact absolute values or measurement error values by T-probe for the swirling flow. Therefore, in this research in the future, additional measurements with an LDA or a multi-hole pressure probe (making it possible to detect a flow direction) will be needed.

Acknowledgment

This work was partially supported by the Fisheries Science Institute of Kunsan National University in 2006. In addition, I would like to thank Mrs. Barbara Baehr and Mr. Wes Hilton for correcting this manuscript grammatically and Prof. Steven G. Buckley of University of California, San Diego in U.S.A. for inviting me as a visiting scholar from Feb. 7, 2006 to Aug. 6, 2007.

References

[1] J. M. Beer and N. A. Chigier, Combustion Aerodynamics, John Wiley & Sons (1972) 102-146.

[2] A. H. Lefebvre, Gas Turbine Combustion, Hemisphere (1983) 126-135.

[3] N. Syred and J. M. Beer, Combustion in Swirling Flows; A Review, *Combustion and Flame* 23 (1974) 143-201.

[4] M. Shioji, I. S. Kim, M. Ikegami and K. Murakami, Flame Stability and NOx Formation in a High-Intensity Swirl Burner, *Trans. JSME (Part B)* 64 (621) (1998) 222-227.

[5] H. Hibara and K. Sudou, Swirling Jet along a Solid Surface, *Trans. JSME (Part B)* 65 (629) (1999) 130-137.

[6] M. S. Feyedelem and T. Sarpkaya, Free- and Near-Free-Surface Swirling Turbulent Jets, *AIAA Journal* 36 (3) (1998) 359-364.

[7] I. Gursul, Effect of Nonaxisymmetric Forcing on a Swirling Jet with Vortex Breakdown, *Trans. ASME, J. of Fluids Eng.* 118 (1996) 316-323.

[8] A. E. Perry, Hot-wire Anemometry, Clarendon Press Oxford (1982).

[9] I. Lekakis, Calibration and Signal Interpretation for Single and Multiple Hot-Wire/Hot-Film Probes, *Meas. Sci. Technol*. 7 (1996) 1313-1333.

[10] L. Lofdahl, Hot-Wire Techniques for the Determination of the Reynolds Stress Tensor in Three-Dimensional Flows, *Dantec Information* (3) (1986).

[11] F. E. Jorgensen, Directional Sensitivity of Wire and Fiber-Film Probes: An Experimental Study, *DISA Information* (11) (1971) 31-37.

[12] C. Gaulier, Measurement of Air Velocity by means of a Triple Hot-Wire Probe, *DISA Information* 21 (1977) 16-20.

[13] J. K. Kim, An Experimental Study on the Three Dimensional Turbulent Flow Characteristics of Swirl Burner for Gas Furnace, *Trans. KSME (Part B),* 25 (2) (2001) 225-234.

[14] J. K. Kim, Investigation of the Three-Dimensional Turbulent Flow Fields of the Gas Swirl Burner with a Cone Type Baffle Plate (Ⅰ), *KSME Int. J.* 15 (7) (2001) 895-905.

[15] J. K. Kim, Experimental Investigation on the Turbulence Augmentation of a Gun-type Gas Burner by Slits and Swirl Vanes, *KSME Int. J.* 18 (10) (2004) 1819-1828.

[16] H. H. Bruun, Hot-Wire Anemometry, Oxford Science Publications (1996) 132-163.

[17] Dantec Dynamics Company, Streamline User's Reference Manual, Chapter 8.3 Algorithms,(2000).

[18] F. H. Champagne and S. Kromat, Experiments on the Formation of a Recirculation Zone in Swirling Coaxial Jets, *Exp. in Fluids* 29 (2000) 494-504.

[19] Dantec Dynamics Company, Mapping 3D-Flows over an offshore helideck, Wind Engineering/ Application Examples (http://www.dantecdyna-mics.com/) (1997-2005).